

# Validation and reproducibility assessment of modality independent elastography in a pre-clinical model of breast cancer

Jared A. Weis<sup>a,b</sup>, Dong Kyu Kim<sup>c</sup>, Thomas E. Yankeelov<sup>a-d</sup>, and Michael I. Miga<sup>a,c,f</sup>  
<sup>a</sup>Vanderbilt University Institute of Imaging Science, <sup>b</sup>Departments of Radiology and Radiological Sciences, <sup>c</sup>Biomedical Engineering, <sup>d</sup>Physics and Astronomy, <sup>e</sup>Cancer Biology, <sup>f</sup>Neurological Surgery, Vanderbilt University, Nashville, TN, USA

## ABSTRACT

Clinical observations have long suggested that cancer progression is accompanied by extracellular matrix remodeling and concomitant increases in mechanical stiffness. Due to the strong association of mechanics and tumor progression, there has been considerable interest in incorporating methodologies to diagnose cancer through the use of mechanical stiffness imaging biomarkers, resulting in commercially available US and MR elastography products. Extension of this approach towards monitoring longitudinal changes in mechanical properties along a course of cancer therapy may provide means for assessing early response to therapy; therefore a systematic study of the elasticity biomarker in characterizing cancer for therapeutic monitoring is needed. The elastography method we employ, modality independent elastography (MIE), can be described as a model-based inverse image-analysis method that reconstructs elasticity images using two acquired image volumes in a pre/post state of compression. In this work, we present preliminary data towards validation and reproducibility assessment of our elasticity biomarker in a pre-clinical model of breast cancer. The goal of this study is to determine the accuracy and reproducibility of MIE and therefore the magnitude of changes required to determine statistical differences during therapy. Our preliminary results suggest that the MIE method can accurately and robustly assess mechanical properties in a pre-clinical system and provide considerable enthusiasm for the extension of this technique towards monitoring therapy-induced changes to breast cancer tissue architecture.

**Keywords:** breast cancer, mechanical properties, elastography, parameter reconstruction, mechanical model

## 1. INTRODUCTION

We have previously introduced a novel elastographic imaging approach capable of transcending murine-to-human length scales while retaining similar loading environments [1]. The method, modality independent elastography (MIE), can be described as a highly translatable model-based inverse image-analysis method that reconstructs elasticity images using two acquired image volumes in a pre/post state of compression. The MIE method represents a novel innovative elastography technique which is automated, simple, amenable to clinical workflow, and able to be implemented consistently across length scales from murine to human. The underlying hypothesis of this work is that elastographic imaging can accurately and reliably monitor therapy-induced changes to breast cancer tissue architecture and as a result become an important therapeutic design tool and prognosticator.

Well-known empirical evidence supports distinct links between the disruption of the normal structural architecture and load-bearing nature of tissue and uncontrolled growth in cancer [2-6]. Elucidation of the mechanobiological basis supporting the association between tumor growth and mechanics continues, with mechanical behavior of the extracellular matrix having been shown to affect growth, differentiation, and motility [7-11]. A strong correlation exists between tissue stiffness and cancer aggressiveness. For example, it has been conclusively demonstrated that accumulation of mechanical stress through increased substrate matrix stiffness inhibits the growth and motility of cancer cells. This response occurs in an aggressiveness dependant manner, with more aggressive cancer cells invading extracellular matrix more effectively than their less aggressive counterparts [12-14]. Processes associated with invadopodia formation, cell contractility, and focal adhesions have been linked to this aggressive behavior, which is affected by the mechanical nature of the extracellular matrix [15, 16].

The emerging elastographic imaging method that we employ shows potential to accurately and reliably monitor tumor progression and therapy-induced changes to breast cancer tissue architecture in both the pre-clinical and clinical settings, and as a result could possibly become an important therapeutic design tool and indicator of response to therapy. Therefore, reliable assessments of the errors associated with this method are critical. In this work, we present preliminary data towards a systematic study of the modality independent elastography (MIE) biomarker towards characterizing cancer mechanical properties for therapeutic monitoring. The goal of this study is to determine the accuracy and reproducibility of MIE and therefore the magnitude of changes required to declare statistical differences during therapy. Preliminary results suggest that the MIE method can accurately and robustly assess mechanical properties in a pre-clinical cancer system and provides considerable enthusiasm for the extension of this technique towards monitoring therapy-induced changes to breast cancer tissue architecture and modulation of the tumor progression/extracellular matrix mechanobiology axis.

## 2. METHODS

### 2.1 MIE approach

The MIE method is an automated image analysis technique that analyzes two anatomical image volumes under differing states of application of mechanical compression. A demons non-rigid registration framework [17] is used to register the post-compression image volume to the pre-compression image volume. Boundary conditions used to drive the biomechanical finite element model during MIE reconstruction are then automatically extracted from the non-rigid registration deformation field. Biomechanical computer models under a Hookean linear elastic assumption are then used to iteratively compress the pre-compression image volume until it matches the acquired post-compression image volume, using an image volume zone-based image correlation coefficient metric. Mechanical property distributions are iteratively reconstructed through the use of a conjugate gradient method with a Polak-Ribière update [18] and an adjoint-based gradient evaluation [19]. Following reconstruction, the output metric is a spatial distribution of mechanical properties. Further details regarding the MIE computational methodology can be found in previous work by our group [20, 21].

Here, MIE is used in a complementary role to traditional magnetic resonance imaging, therefore *a priori* MR signal intensity information from the  $T_2$  weighted anatomical MR image volume is used to group tissues of interest for property reconstruction. A  $k$ -means clustering algorithm with the application of a Markov random field spatial constraint is used to classify separate tissues of interest based on MR signal intensity information. As the Markov random field models the spatial interactions within the image volume, this imposes spatial continuity to the clustering step and produces more robust results than traditional  $k$ -means clustering alone. Following tissue classification, regions for subsequent mechanical property reconstruction are identified through geometrical sub-clustering of the identified tissue classes, where the number and size of geometrical sub-clusters (regions) defines the reconstruction resolution. Figure 1 shows the output of the individual processing steps for a murine MIE dataset, from anatomical MR images to reconstructed elasticity ratios.

Similar to the work by McGarry et al. [22], here, prior information is used as a ‘soft’ constraint, with a weighted penalty function applied to the calculated gradient, which is used to drive iterative updates to the spatial elasticity during reconstruction, that enforces similar mechanical properties in regions belonging to similar tissue classes. This constraint acts to penalize large deviations within a tissue type *via* identified spatial priors. This soft prior constraint is enforced using Eqs. 1 and 2:

$$g_s = g - \beta L^T g \quad [1]$$

$$L_{i,j} = \begin{bmatrix} -1/n-1 \\ 1 \\ 0 \end{bmatrix} \quad \begin{array}{l} \text{region}_i = \text{region}_j \\ i=j \\ \text{otherwise} \end{array} \quad [2]$$

Where  $g_s$  is the soft prior penalized gradient,  $g$  is the calculated gradient,  $\beta$  is the empirically selected strength of the soft prior weighting constraint, and is defined in the range of  $[0,1]$  with 0 is no prior constraint and 1 is a hard prior constraint.  $L$  is an  $n \times n$  matrix, where  $n$  is the number of reconstruction regions.

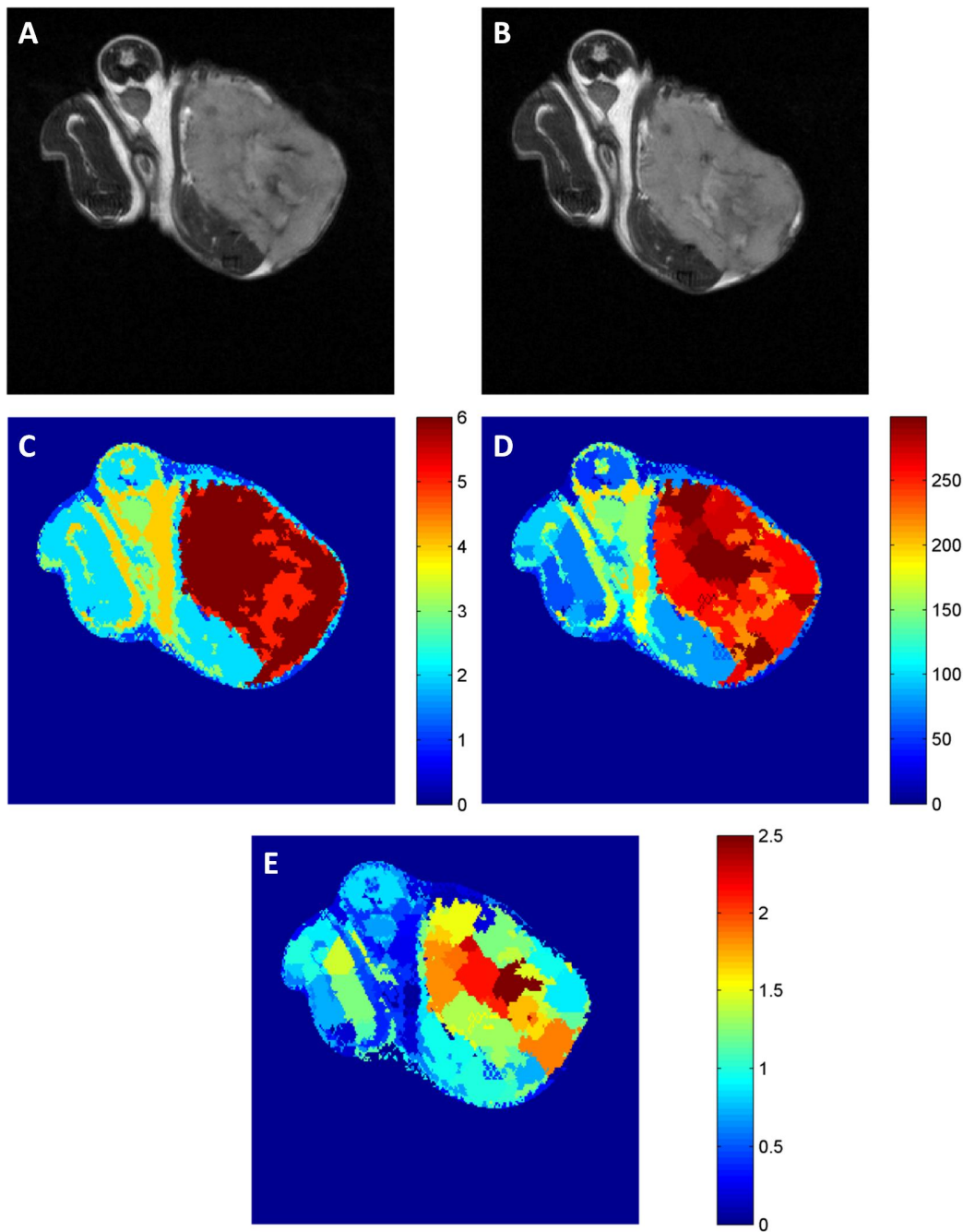


**Figure 1.** Processing steps for a murine MIE dataset. Uncompressed (A) and compressed (B) anatomical MR image volumes are acquired. Spatially constrained  $k$ -means clustering with Markov random fields is used to classify tissues of interest (C) for *a priori* constraints. Regions for property reconstruction are defined by geometrical sub-clustering (D). A finite element model is built and the MIE elasticity reconstruction (E) is iteratively computed.

## 2.2 Gel phantom data

Preliminary evaluation of the accuracy of the MIE imaging method was performed using a poly-vinyl alcohol cyrogel (PVAC) phantom with two different material properties, as determined by the number of freeze-thaw cycles (FTC) the material underwent. The phantom was created using a layered construction with two gadolinium-doped stiff layers (two FTC's) on the top and bottom of one soft layer (one FTC). Phantoms were created with a diameter of approximately 22 mm and height of approximately 13 mm.  $T_2$  weighted MR image volumes were acquired before and after the application of compression by a 5cc balloon catheter controlled by a syringe driver placed within the MR imaging coil. MRI was performed using a Varian 7.0T scanner (Varian, Palo Alto, CA) with a 38-mm quadrature coil and were acquired using a fast spin echo sequence. Semi-automatic image segmentation was used to identify the two material types in the uncompressed image volume and the MIE method was used to estimate elastic property contrast between each material as described above. Separate samples of both the inclusion and background gel material were subjected to material testing using an Enduratec Electroforce 3100 mechanical tester (Bose, Enduratec Systems Group, Minnetonka, MN) for independent evaluation of the reconstructed stiffness ratio.

## 2.3 Murine data

A murine xenograft pre-clinical model of triple-negative breast cancer was used where 4 to 6 week old female athymic nude mice (Harlan, Indianapolis, IN) were injected subcutaneously in the right flank with approximately  $10^7$  MDA-MB-231 cells in a 30% Matrigel suspension. Tumors were allowed to grow for 8-10 weeks. MRI anatomical  $T_2$  weighted image volumes were acquired using a Varian 7.0T scanner (Varian, Palo Alto, CA) with a 38-mm quadrature coil. Anatomical images were acquired before and after compression using a fast spin echo sequence. Compression was applied by a 5cc balloon catheter controlled by a syringe driver that was placed within the MR imaging coil in close proximity to the tumor. Assessment of reproducibility was performed using a test/re-test approach, where animals were removed between scans and allowed to recover in order to simulate the normal repositioning of an animal that occurs during a longitudinal treatment study. All animal procedures were approved by the Vanderbilt University Institutional Animal Care and Use Committee.

## 3. RESULTS

MIE validation was performed in PVAC phantoms representing a stiff inclusion layer encapsulated between soft layers. Structural MR image volumes acquired before (Figure 2A) and after (Figure 2B) the application of compression were used to estimate relative elastic property contrast between each material (Figure 2C). The MIE method is shown to reconstruct an estimated elastic property contrast ratio between the stiff and soft material layers of 26.8 to 1, whereas independent mechanical testing reveals a ratio of 27.4 to 1. Using mechanical testing as the gold standard, this represents ~2.5% error in the accuracy of the MIE measurement for this investigation. It is important to note that the MIE method provides a full three-dimensional reconstruction of the relative elastic properties in the sample of interest. Here, we show two-dimensional central-slice images to represent the entire sample.

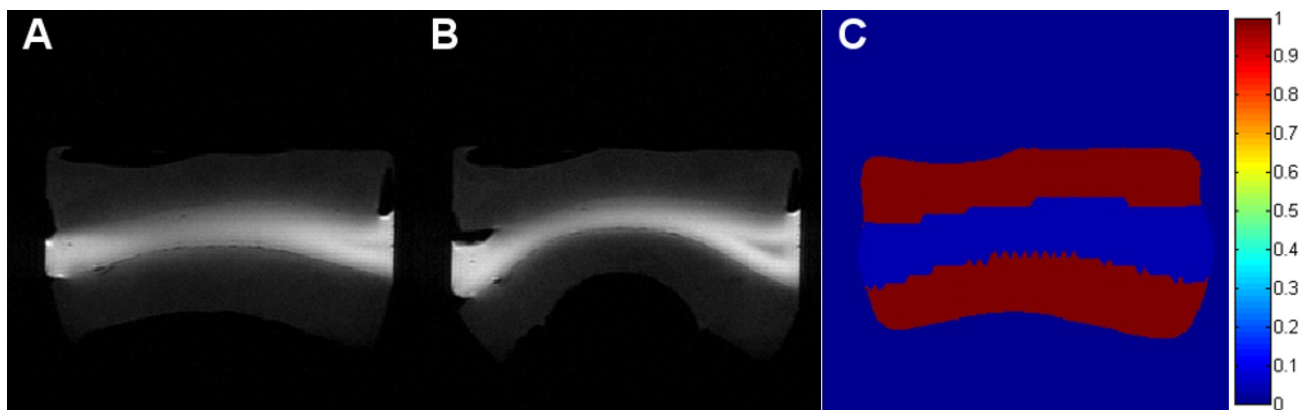


**Figure 2.** Pre (A) and post (B) compression MR data and respective MIE reconstruction elastic property contrast map (C) for the two property PVAC phantom validation experiment.

Test/re-test reproducibility assessment of the MIE elasticity biomarker was performed by analyzing mechanical properties of murine tumors from two different sets of scans performed on the same animal at the same day, separated by a short recovery period. During this recovery period, animals were removed and allowed to recover prior to repeating the scan. This simulates the normal repositioning of an animal that would occur during a longitudinal treatment study to assess response to therapy. Figure 3 shows uncompressed images (Figure 3A, B) and corresponding MIE reconstructions (Figure 3C, D) from similar slices for each scan in the test/re-test reproducibility dataset from one animal. To facilitate side-by-side comparisons of MIE reconstruction results from individual test/re-test assessments of the same subject, adjacent muscle tissue was used as an internal reference property and the reconstructed elastic property contrast map was scaled to unity for the identified reference material. Tumor periphery-to-muscle elastic property ratio in each analysis was approximately 1.89 to 1 and 1.84 to 1, representing 2.7% test/re-test reproducibility error in this assessment.

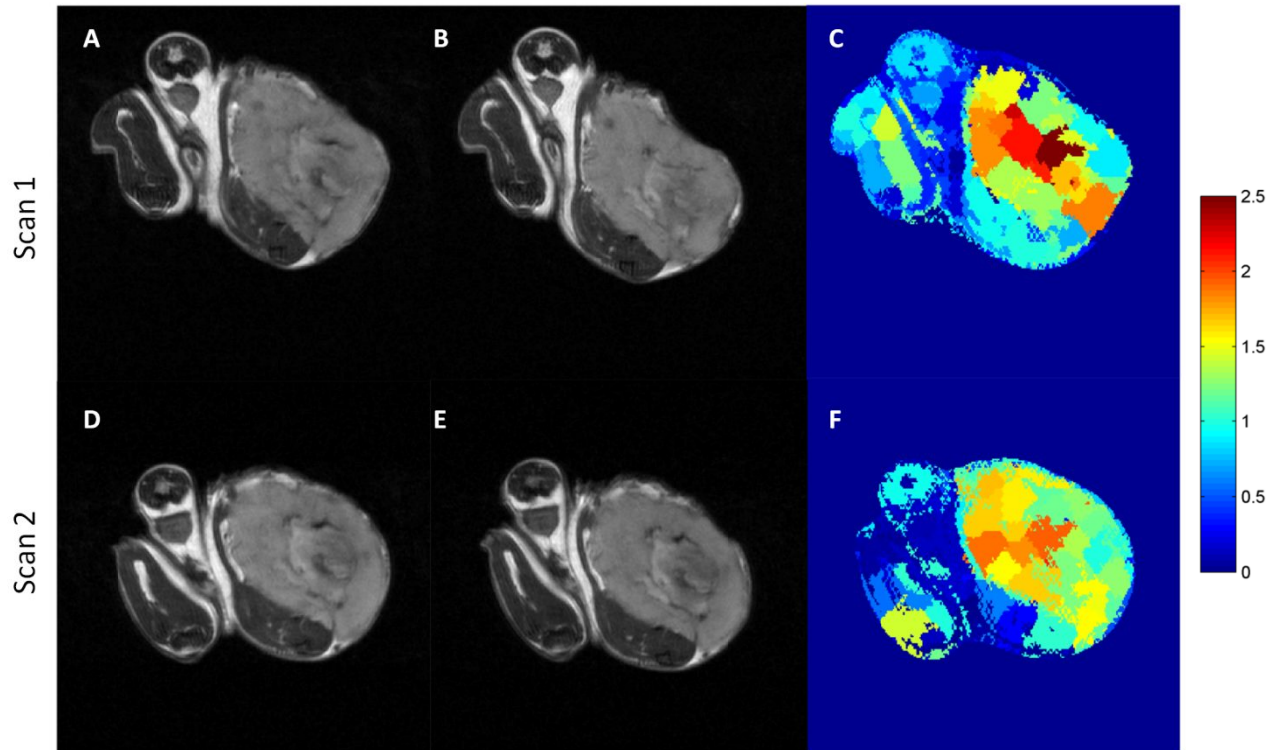


**Figure 3.** Test/re-test repeatability assessment of the MIE method from two assessments (A-C) and (D-F) of the same mouse, showing reproducibility of the MIE measurement. Uncompressed MR data (A,D), compressed MR data (B,E) and corresponding MIE reconstructions (C,F).

#### 4. CONCLUSIONS

MIE has been under investigation for several years [20, 21, 23-26], however a systematic study of the error associated with the methodology has yet to be undertaken. Recent breakthroughs towards automation, translation, and consistent application in the pre-clinical cancer setting [1] have fundamentally improved its possible use as an elasticity biomarker. In this work, we demonstrate an initial realization towards a systematic study of the MIE elasticity biomarker in characterizing mechanical properties of cancer for therapeutic monitoring. The MIE method is shown to report an elasticity biomarker that is highly accurate and reproducible in a pre-clinical model of breast cancer. This initial assessment of accuracy and reproducibility of MIE provides considerable excitement for future work towards design, monitoring, and prediction of outcomes for therapeutic agents in the modulation of the tumor progression/extracellular matrix mechanics axis. While preliminary, assessment of the accuracy and reproducibility of MIE are shown, and

provides guidance on the magnitude of changes required to declare significant statistical differences in tissue elasticity assessed by MIE during therapy. Future work will involve a robust statistical analysis of the repeatability index through analysis of more quantitative reproducibility assessment data.

## ACKNOWLEDGEMENTS

This work was supported by the National Institutes of Health, the National Cancer Institute by R01CA138599, R25CA092043, U01CA142565, and U01CA174706. This work was also supported by the Vanderbilt initiative in Surgery and Engineering Pilot Award Program.

## REFERENCES

- [1] Weis, J. A., Yankeelov, T. E., Munoz, S. A., Sastry, R. A., Barnes, S. L., Arlinghaus, L. R., Li, X., and I., M. M. "A consistent pre-clinical/clinical elastography approach for assessing tumor mechanical properties in therapeutic systems," SPIE 2013 Medical Imaging: Biomedical Applications in Molecular, Structural, and Functional Imaging (2013).
- [2] Paszek, M. J. and Weaver, V. M., "The tension mounts: mechanics meets morphogenesis and malignancy," *J Mammary Gland Biol Neoplasia*, vol. 9(4), p. 325-42 (2004).
- [3] Paszek, M. J., Zahir, N., Johnson, K. R., Lakins, J. N., Rozenberg, G. I., Gefen, A., Reinhart-King, C. A., Margulies, S. S., Dembo, M., Boettiger, D., Hammer, D. A., and Weaver, V. M., "Tensional homeostasis and the malignant phenotype," *Cancer Cell*, vol. 8(3), p. 241-54 (2005).
- [4] Paszek, M. J., Zahir, N., Lakins, J. N., Johnson, K., Rozenberg, G., Dembo, M., Hammer, D. A., and Weaver, V. M., "Mechano-signaling in mammary morphogenesis and tumorigenesis," *Molecular Biology of the Cell*, vol. 15p. 241a-241a (2004).
- [5] Huang, S. and Ingber, D. E., "Cell tension, matrix mechanics, and cancer development," *Cancer Cell*, vol. 8(3), p. 175-176 (2005).
- [6] Shieh, A. C., "Biomechanical forces shape the tumor microenvironment," *Ann Biomed Eng*, vol. 39(5), p. 1379-89 (2011).
- [7] Engler, A. J., Berry, M., Sweeney, H. L., and Discher, D. E., "Substrate compliance alters human mesenchymal stem cell morphology," *Molecular Biology of the Cell*, vol. 15p. 298a-298a (2004).
- [8] Engler, A. J., Feng, H., Sweeney, H. L., and Discher, D. E., "Cells on gels: Skeletal muscle cell differentiation and adhesion on flexible substrates," *Molecular Biology of the Cell*, vol. 13p. 63a-63a (2002).
- [9] Engler, A. J., Berry, M., Sweeney, H. L., and Discher, D. E., "Substrate elasticity directs adult mesenchymal stem cell differentiation," *Biorheology*, vol. 42(1-2), p. 33-33 (2005).
- [10] Lo, C. M., Wang, H. B., Dembo, M., and Wang, Y. L., "Cell movement is guided by the rigidity of the substrate," *Biophysical Journal*, vol. 79(1), p. 144-152 (2000).
- [11] Yeung, T., Georges, P. C., Flanagan, L. A., Marg, B., Ortiz, M., Funaki, M., Zahir, N., Ming, W. Y., Weaver, V., and Janmey, P. A., "Effects of substrate stiffness on cell morphology, cytoskeletal structure, and adhesion," *Cell Motility and the Cytoskeleton*, vol. 60(1), p. 24-34 (2005).
- [12] Helmlinger, G., Netti, P. A., Lichtenbeld, H. C., Melder, R. J., and Jain, R. K., "Solid stress inhibits the growth of multicellular tumor spheroids," *Nature Biotechnology*, vol. 15(8), p. 778-783 (1997).
- [13] Stein, A. M., Demuth, T., Mobley, D., Berens, M., and Sander, L. M., "A mathematical model of glioblastoma tumor spheroid invasion in a three-dimensional in vitro experiment," *Biophysical Journal*, vol. 92(1), p. 356-365 (2007).
- [14] Cheng, G., Tse, J., Jain, R. K., and Munn, L. L., "Micro-environmental mechanical stress controls tumor spheroid size and morphology by suppressing proliferation and inducing apoptosis in cancer cells," *PLoS One*, vol. 4(2), p. e4632 (2009).
- [15] Burridge, K. and Doughman, R., "Front and back by Rho and Rac," *Nat Cell Biol*, vol. 8(8), p. 781-2 (2006).
- [16] Roovers, K. and Assoian, R. K., "Effects of rho kinase and actin stress fibers on sustained extracellular signal-regulated kinase activity and activation of G(1) phase cyclin-dependent kinases," *Mol Cell Biol*, vol. 23(12), p. 4283-94 (2003).

- [17] Thirion, J. P., "Image matching as a diffusion process: an analogy with Maxwell's demons," *Med Image Anal*, vol. 2(3), p. 243-60 (1998).
- [18] Polak, E. and Ribiere, G., "Note sur la convergence des méthodes de directions conjuguées," *Rev. Fr. Inform. Rech. Oper.*, vol. 16p. 35-43 (1969).
- [19] Oberai, A. A., Gokhale, N. H., and Feijoo, G. R., "Solution of inverse problems in elasticity imaging using the adjoint method," *Inverse Problems*, vol. 19p. 297-313 (2003).
- [20] Ou, J. J., Ong, R. E., Yankeelov, T. E., and Miga, M. I., "Evaluation of 3D modality-independent elastography for breast imaging: a simulation study," *Physics in Medicine and Biology*, vol. 53(1), p. 147-163 (2008).
- [21] Pheiffer, T. S., Ou, J. J., Ong, R. E., and Miga, M. I., "Automatic Generation of Boundary Conditions Using Demons Nonrigid Image Registration for Use in 3-D Modality-Independent Elastography," *Ieee Transactions on Biomedical Engineering*, vol. 58(9), p. 2607-2616 (2011).
- [22] McGarry, M., Johnson, C. L., Sutton, B. P., Van Houten, E. E., Georgiadis, J. G., Weaver, J. B., and Paulsen, K. D., "Including spatial information in nonlinear inversion MR elastography using soft prior regularization," *IEEE Trans Med Imaging*, vol. 32(10), p. 1901-9 (2013).
- [23] Miga, M. I., "A new approach to elastographic imaging: Modality independent elastography," *Medical Imaging 2002: Image Processing: Proc. of the SPIE*, vol. 4684p. 604-611 (2002).
- [24] Miga, M. I., "A new approach to elastography using mutual information and finite elements," *Phys Med Biol*, vol. 48(4), p. 467-80 (2003).
- [25] Miga, M. I., Rothney, M. P., and Ou, J. J., "Modality independent elastography (MIE): Potential applications in dermoscopy," *Medical Physics*, vol. 32(5), p. 1308-1320 (2005).
- [26] Washington, C. W. and Miga, M. I., "Modality independent elastography (MIE): A new approach to elasticity imaging," *Ieee Transactions on Medical Imaging*, vol. 23(9), p. 1117-1128 (2004).